Zoological Letters

RESEARCH ARTICLE

Open Access

Photoreceptor genes in a trechine beetle, *Trechiama kuznetsovi*, living in the upper hypogean zone

Takuma Niida[1*], Yuto Terashima[1], Hitoshi Aonuma[2] and Shigeyuki Koshikawa[1,3*]

Abstract

To address how organisms adapt to a new environment, subterranean organisms whose ancestors colonized subterranean habitats from surface habitats have been studied. Photoreception abilities have been shown to have degenerated in organisms living in caves and calcrete aquifers. Meanwhile, the organisms living in a shallow subterranean environment, which are inferred to reflect an intermediate stage in an evolutionary pathway to colonization of a deeper subterranean environment, have not been studied well. In the present study, we examined the photoreception ability in a trechine beetle, *Trechiama kuznetsovi*, which inhabits the upper hypogean zone and has a vestigial compound eye. By de novo assembly of genome and transcript sequences, we were able to identify photoreceptor genes and phototransduction genes. Specifically, we focused on *opsin* genes, where one *long wavelength opsin* gene and one *ultraviolet opsin* gene were identified. The encoded amino acid sequences had neither a premature stop codon nor a frameshift mutation, and appeared to be subject to purifying selection. Subsequently, we examined the internal structure of the compound eye and nerve tissue in the adult head, and found potential photoreceptor cells in the compound eye and nerve bundle connected to the brain. The present findings suggest that *T. kuznetsovi* has retained the ability of photoreception. This species represents a transitional stage of vision, in which the compound eye regresses, but it may retain the ability of photoreception using the vestigial eye.

Keywords Blind ground beetle, Adaptation, Evolution, Carabidae, Mesovoid shallow substratum

Background

How organisms adapt to a new environment is one of the fundamental research questions in evolutionary biology [1]. Subterranean organisms whose ancestors originally lived in a surface environment are ideal for investigating this issue [2, 3]. Subterranean habitats are not continuously exposed to light, and can be categorized into cave habitats, interstitial habitats and superficial subterranean habitats [4, 5]. Degeneration of eyes is generally observed in various taxa colonizing these subterranean environments [6, 7].

Do the organisms having a regressed eye also have decreased ability of photoreception? Previous studies focused on various aspects of subterranean adaptation, including signatures in photoreceptor proteins [8, 9]. For example, one previous study described the expression of visual opsin genes which encode seven-transmembrane photoreceptor proteins in the binocular eye of the Mexican blind cavefish, *Astyanax mexicanus* [8]. Transcripts of visual opsin genes were

*Correspondence:
Takuma Niida
ymbnw8bwgmxikb91sqck@gmail.com
Shigeyuki Koshikawa
koshi@ees.hokudai.ac.jp
[1] Graduate School of Environmental Science, Hokkaido University, Sapporo, Japan
[2] Department of Biology, Graduate School of Science, Kobe University, Kobe, Japan
[3] Faculty of Environmental Earth Science, Hokkaido University, Sapporo, Japan

underrepresented in the cavefish as compared with a conspecific surface population, and this could be attributed to reduction of photoreceptor cells in the cavefish [10]. In other examples, a blind mole rat has an ultraviolet-sensitive/violet-sensitive opsin gene with deleterious mutations, and fossorial snakes with reduced eyes, Scolecophidia, did not have visual opsin genes in the genome or transcripts [11, 12].

In Insecta, subterranean diving beetles (Dytiscidae), which have highly regressed or no eyes and inhabit a calcrete aquifer located 10 m underground in Western Australia, were subjected to a similar analysis [13]. Transcripts were not detected for *long wavelength opsin* or *ultraviolet opsin* at the adult stage of the diving beetles [14], and pseudogenization of *long wavelength opsin*, *ultraviolet opsin* and some phototransduction genes was observed [15, 16].

Besides calcrete aquifers, insects have also been found to colonize superficial subterranean habitats, such as rock fissures near the surface [17]. Insects living in a superficial subterranean habitat can be exposed to light due to unexpected environmental fluctuation. The colonization of a superficial subterranean habitat is inferred to reflect an intermediate stage in an evolutionary pathway to colonization of deeper and extreme environments [4]. Despite this importance, the biological features of species living in a superficial subterranean habitat remain unexplored.

The present study focused on one trechine beetle species, *Trechiama kuznetsovi* (Coleoptera: Carabidae: Trechinae). This species has a vestigial compound eye and inhabits the upper hypogean zone, which is a similar environment to mesovoid shallow substratum (MSS). The habitat of the type specimens was either under stones or soil deposits along narrow streams [18]. We aimed to reveal the photoreception ability in this species. We obtained genome and transcript sequences to examine photoreceptor genes and phototransduction genes and estimate selective pressure on visual opsin genes. Also, histological investigations were performed to observe the internal structure of the vestigial compound eye and a nerve bundle connecting it to the brain.

Methods

Sample collection

Trechiama kuznetsovi samples were collected at Yûbari City, Hokkaido, Japan. We collected *T. kuznetsovi* adults from the upper hypogean zone consisting of small rocks and clay, by digging and finding by sight in the slope of a v-shaped valley to the depth of a few to some dozen centimeters (Fig. 1).

DNA and RNA sequencing

We used one adult male of *T. kuznetsovi* stored in 99.5% ethanol for genome sequencing. Before DNA extraction, mites adhering to the body surface were removed and the male genitalia was preserved in 99.5% ethanol for identification. Genomic DNA was extracted using a Wizard Genomic DNA Purification Kit (Promega, Madison, WI, USA). A library was constructed using a TruSeq Nano DNA Library Prep Kit (Illumina, San Diego, CA, USA) and sequenced on the NovaSeq 6000 platform (Illumina) by Macrogen Service (Macrogen, Seoul, South Korea). 2×151 bp paired-end reads were generated (Table S1).

We used one live adult male of *T. kuznetsovi* for transcript sequencing. Before RNA extraction, the beetle was washed with 99.5% ethanol, mites adhering on its body surface were removed and the male genitalia was preserved in 99.5% ethanol for identification. Total RNA was immediately extracted from the whole body using an RNeasy Micro Kit (Qiagen, Hilden, Germany) since vestigial compound eyes were too small to extract RNA and construct a library for sequencing. A library was constructed using a SMARTer Stranded RNA-Seq Kit (Illumina) and sequenced on the NovaSeq 6000 platform (Illumina) by Macrogen Service. 2×101 bp paired-end reads were generated (Table S1).

Assembly and mapping

Summary statistics of raw reads and adapter contamination were checked using FastQC (v0.11.9; Babraham Institute). Quality control was performed using fastp v0.20.1 [19] and Trimmomatic v0.39 [20] to trim off one base from the 3′ end, low quality sequences and adapter sequences. Then, summary statistics were rechecked using FastQC. The kmer content of reads from genome sequencing and the genome size were calculated using KmerGenie v1.7051 [21]. For the reads that passed the quality control, genome and transcript assembly were conducted with Platanus v1.2.4 [22] and Trinity v2.8.4 [23, 24]. Before the scaffolding step of genome assembly, contigs smaller than 500 bp were excluded [25]. Completeness of the assembled genome and transcript was assessed using BUSCO_v5 for insecta core gene sets and CEGMA for invertebrate core gene sets in gVolante web server [26]. Summary statistics of the assembled sequences were calculated using SeqKit v.0.16.1 [27].

RNA reads were mapped to the assembled genome scaffolds using HISAT v2.1.0 [28]. The result of the mapping was visualized using IGV v2.11.9 [29].

Homology search

We conducted a search for genes encoding three photoreceptor proteins and 15 phototransduction proteins from

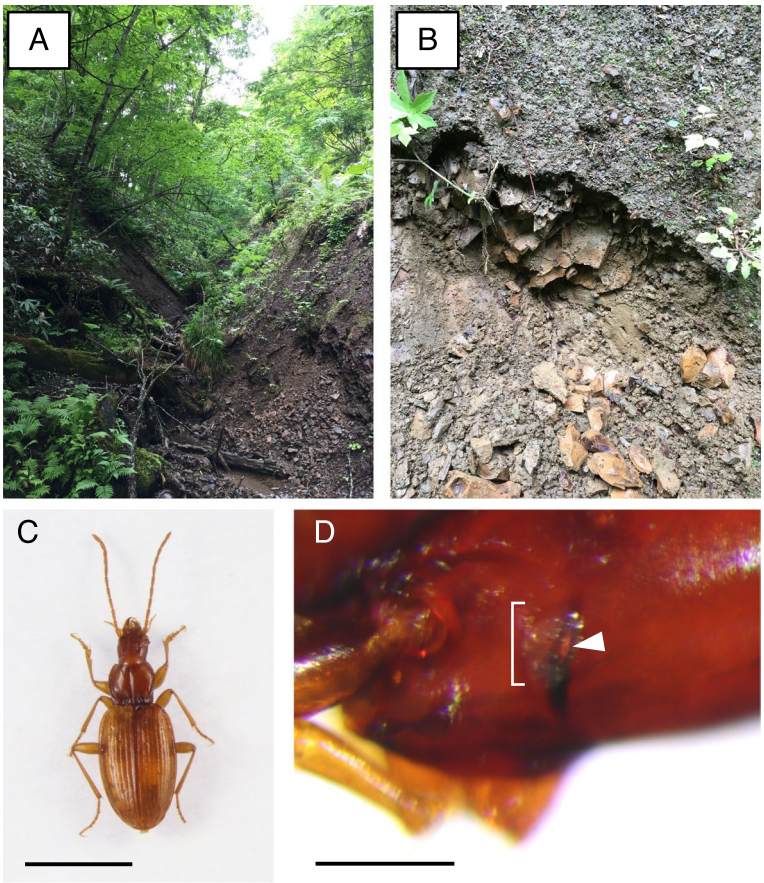

Fig. 1 The habitat and morphology of *T. kuznetsovi*. **A** A v-shaped valley of a mountain area at Yûbari City in Hokkaido. **B** The upper hypogean zone under the slope of a v-shaped valley. It consists of small rocks and clay. **C** Dorsal view of *T. kuznetsovi*. Scale bar indicates 3 mm. **D** Lateral view of *T. kuznetsovi* head. The bracket indicates the vestigial compound eye. The black part is the pigmentation of the cuticle behind a compound eye (ocular ridge). The arrowhead indicates a hole on the ocular ridge, through which the nerve bundle is presumed to pass. There is no pigmentation in cells inside the compound eye structure. Scale bar indicates 0.2 mm

the assembled genome and transcripts with the tblastn program using the following queries (unless noted, protein sequences of *Tribolium castaneum* [Tenebrionidae] were used): Long wavelength opsin (Lw opsin) of *Pogonus chalceus* (Carabidae: Trechinae), Ultraviolet opsin (Uv opsin) of *P. chalceus*, C-opsin, Arrestin 1 (Arr1), Arrestin 2 (Arr2), G protein α-subunit 49B (Gα49B), G protein β-subunit 76C (Gβ76C), G protein γ-subunit 30A (Gγ30A), G protein-coupled receptor kinase 1 (Gprk1), Inactivation no afterpotential D (InaD), Neither inactivation nor afterpotential A (NinaA), Neither inactivation nor afterpotential C (NinaC), No receptor potential A (NorpA), Protein C kinase 53E (Pkc53E) of *Drosophila melanogaster*, Rab-protein 6 (Rab6), Retinal degeneration C (RdgC), Transient receptor potential (Trp), and Trp-like (Trpl). Only two types of visual opsin proteins (Uv opsin and Lw opsin) were known in Coleoptera [30]. The selection of the other proteins was based on previous studies [31, 32]. Blast-hit sequences with an e-value $<1\times e^{-20}$ were treated as having high similarity [33]. If no sequence matched this criterion, Blast-hit sequences were examined in order from the best-hit sequence. In BLAST-search for the transcripts, the presence of premature stop codons and frameshift mutations was examined.

We subsequently conducted a further analysis of *lw opsin* and *uv opsin*, which are visual photoreceptor genes in Coleoptera, while some opsin genes are known to have light-independent roles in *D. melanogaster* [30, 34–37]. We checked whether the blast-hit transcripts matched exon regions with mapped short reads of transcripts using HISAT. Matched transcripts were used for subsequent comparative analyses with a related surface species: *P. chalceus*, whose opsin amino acid sequences were already registered in NCBI protein database [30].

Identification of *lw opsin* gene

A part of the genome sequence that had high similarity score to the Lw opsin amino acid sequence of *P. chalceus* in a tblastn search was divided into three scaffolds (Table S2). To join these scaffolds together, primers were designed on each scaffold using Primer3Plus (https://www.bioinformatics.nl/cgi-bin/primer3plus/primer3plus.cgi) (Table S3) and PCR was performed using PrimeSTAR Max DNA Polymerase (Takara Bio, Shiga, Japan). The sequences of the PCR products, which were determined by Sanger sequencing, were overlapped on the scaffolds. The transcript sequence that had a high similarity score to the Lw opsin amino acid sequence of *P. chalceus* in a tblastn search was divided into two contigs assembled by Trinity (Table S2). It is generally difficult to assemble transcripts expressed at low levels into a single contig [38]. These contigs were joined together by Sanger sequencing using the same method as above. Primers were designed on each contig (Table S3) and RT-PCR was performed using a 3′ RACE CORE Set (Takara Bio).

To specify exon and intron regions, the acquired transcript sequence of the *lw opsin* gene was aligned to the acquired genome sequence of the *lw opsin* gene with Exonerate v2.4.0 [39]. The exon and intron regions were illustrated with GenePalette [40].

Identification of *uv opsin* gene

There was one genome scaffold that had high similarity score to the Uv opsin amino acid sequence of *P. chalceus* in a tblastn search (Table S2), but no transcript contig was found. However, short read sequences originated from RNA sequencing were mapped to the scaffold of the *uv opsin* gene. This means that the *uv opsin* gene was expressed and short reads derived from mRNA were detected as a result of RNA sequencing, but not correctly assembled by Trinity, probably because of the low number of reads. We determined the transcript sequence of the *uv opsin* gene by Sanger sequencing. Firstly, the exon regions were predicted with Exonerate using the Uv opsin amino acid sequence of *P. chalceus*. Then primers were designed on the predicted exon regions with Primer3Plus (Table S3) and RT-PCR was performed using a 3′ RACE CORE Set.

To specify exon and intron regions, the acquired transcript sequence of the *uv opsin* gene was aligned to the acquired genome sequence of the *uv opsin* gene with Exonerate. The exon and intron regions were illustrated with GenePalette.

Opsin phylogeny and tests of selection

Blastp was performed using the acquired amino acid sequences of opsins in *T. kuznetsovi* as queries for non-redundant protein sequences in the NCBI database (Table S4). Amino acid sequences of opsins in *T. kuznetsovi*, four beetle species (*P. chalceus*, *Gyrinus marinus*, *Thermonectus marmoratus* and *T. castaneum*) and a honeybee (*Apis mellifera*) were aligned with MUSCLE in MEGA v 11 [41]. Based on the maximum likelihood method, a phylogenetic tree of nucleotide sequences was reconstructed under the best-fit GTR + G + I model with 1000 bootstrap generations.

The ancestral sequences of opsin gene sequences between subterranean *T. kuznetsovi* and surface *P. chalceus* were estimated, based on the above five beetles' phylogenetic relationship using MEGA. Based on the maximum likelihood method [42], the ratios of nonsynonymous (Ka) to synonymous (Ks) nucleotide substitution rates were calculated between an ancestral sequence and a sequence of *T. kuznetsovi* and between the ancestor sequence and a sequence of *P. chalceus* using KaKs_Calculator v 3.0 [43]. Fisher's exact test on a 2 × 2 contingency table was conducted using the number of synonymous and nonsynonymous sites and synonymous and nonsynonymous substitutions.

The Ka/Ks analysis is able to suggest that observed changes in a sequence have been influenced by positive selection (Ka/Ks > 1), neutral evolution (Ka/Ks = 1), or negative (purifying) selection (Ka/Ks < 1). In our study, the apparent result is expected to be that opsin genes of *T. kuznetsovi* were under purifying selection, because along the evolutionary branch from an ancestor to *T. kuznetsovi*, opsins will have been selected under surface habitat before this lineage colonized subterranean habitat. To resolve this problem, we also compared the degrees of purifying selection between opsin genes of *T. kuznetsovi* (test) and *P. chalceus* (reference), carrying out branch-by-branch analyses with RELAX in Hyphy [44]. As the result of this model, $k < 1$ is indicative of relaxed selection, while $k > 1$ is indicative of purifying selection.

Histological study

The internal structure of a vestigial compound eye in *T. kuznetsovi* adults was observed using paraffin sections. Adult heads were fixed in 50% alcohol Bouin solution (ethanol:Bouin solution [for pathology, Fujifilm Wako Pure Chemicals] = 1:1) at room temperature overnight or longer. The fixed samples were rinsed in 70% ethanol, dehydrated in increasing concentrations of ethanol (90, 95 and 100%) [45, 46], and then cleared in xylene. Next, the samples were embedded in paraffin (Paraplast Plus; Sigma Aldrich, MO, USA), and transverse sections (6 μm) were serially cut with a microtome (OSK 97LF506; Ogawa Seiki, Tokyo, Japan). Sections were stained with hematoxylin, observed with a microscope (CX-43; OLYMPUS, Tokyo, Japan) and

photographed with a mounted camera (EOS Kiss X9; Canon, Tokyo, Japan).

Because we could not obtain the complete series of cross sections due to their friability, the nerve bundle between a compound eye and a brain in *T. kuznetsovi* adults was observed with dissection. Adult heads were dissected in phosphate-buffered saline and stained with 0.5% methylene blue solution (22409-32; Nakalai Tesque, Kyoto, Japan) for 1 h. The samples were washed in phosphate-buffered saline, observed with a stereo microscope (SZX16; OLYMPUS) and photographed with a mounted camera (EOS Kiss X9; Canon).

Results

DNA and RNA sequencing

The genome size was estimated to be 554,652,206 bp based on the k-mer frequency distribution of genome reads with KmerGenie. The assembled genome contained 55,616 scaffolds with a total length of 456,726,283 bp (N50: 16,592 bp) and 96.20% BUSCO completeness (Table 1). The assembled transcripts contained 71,303 contigs with a total length of 67,456,903 bp (N50: 1,883 bp) and 89.10% BUSCO completeness (Table 1). 81.90% of RNA reads were mapped to the assembled genome with HISAT. The information of paired-end reads is summarized in Table S1.

Expression of photoreceptor genes and phototransduction genes

In the assembled genome, BLAST search found *lw opsin* gene, *uv opsin* gene and non-visual *c-opsin* gene (Table 2). *lw opsin* and *c-opsin* were found in the assembled transcripts, but *uv opsin* was not. Fifteen BLAST-searched phototransduction genes were found in the assembled genome. Out of those, transcripts for 14 BLAST-searched phototransduction genes were detected, namely, *Arr1*, *Arr2*, *Gα49B*, *Gβ76C*, *Gγ30A*, *Gprk1*, *inaD*, *ninaA*, *ninaC*, *norpA*, *Pkc53E*, *Rab6*, *rdgC* and *trp*. Most of these transcript sequences had neither a premature stop codon nor a frameshift mutation, but transcript sequences of *Gα49B*, *Gβ76C*, *Gprk1*, *norpA* and *rdgC* included apparent functional isoforms and those with premature stop codons or frameshift mutations. These transcripts might include primary transcripts before splicing. One phototransduction gene, *trpl*, was not detected in the Trinity-assembled transcripts. Short read sequences obtained by RNA sequencing were mapped to the genome scaffold of the *trpl* gene. We performed an additional RT-PCR experiment, but no clear PCR product was observed. This probably means that the *trpl* gene was expressed at a very low level.

Table 1 The summary statistics for assembly of the genome and transcripts in *T. kuznetsovi*

	Genome	Transcripts
Total assembled length (bp)	456,726,283	67,456,903
Scaffolds (n)	55,616	71,303
The longest scaffold (bp)	306,214	52,805
The shortest scaffold (bp)	386	181
Scaffold N50 (bp)	16,592	1,883
BUSCO pipeline analysis (% complete / partial)	96.20 / 98.83	89.10 / 95.32
CEGMA pipeline analysis (% complete / partial)	93.55 / 100	Not Available

Table 2 Photoreceptor and phototransduction genes detected in the assembled genome and transcripts

Query			*T. kuznetsovi*	
Protein name	**Species**	**Accession no**	**Genome**	**Transcripts**
Visual opsin proteins				
Lw opsin	Pcha	APY20654	yes	yes (+)
Uv opsin	Pcha	APY20653	yes	no[a]
Non-visual opsin protein				
C-opsin	Tcas	NP_001138950	yes	yes (+)
Phototransduction proteins				
Arr1	Tcas	XP_966595	yes	yes (+)
Arr2	Tcas	NP_001164084	yes	yes (+)
Gα49B	Tcas	XP_966311	yes	yes (+/–)
Gβ76C	Tcas	XP_973851	yes	yes (+/–)
Gγ30A	Tcas	XP_972123	yes*	yes (+)
Gprk1	Tcas	XP_966480	yes	yes (+/–)
InaD	Tcas	XP_015837295	yes	yes (+)
NinaA	Tcas	XP_973192	yes	yes (+)
NinaC	Tcas	XP_015835531	yes	yes (+)
NorpA	Tcas	XP_001812780	yes	yes (+/–)
Pkc53E	Dmel	NP_476682	yes	yes (+)
Rab6	Tcas	XP_972453	yes	yes (+)
RdgC	Tcas	XP_974915	yes	yes (+/–)
Trp	Tcas	XP_968670	yes	yes (+)
Trpl	Tcas	XP_968598	yes	no[b]

'yes' indicates that the genes were detected at e-value $< 1 \times e^{-20}$. 'yes*' indicates that the gene was detected at e-value $\geq 1 \times e^{-20}$. 'no' indicates that the genes were not detected in BLAST-hit sequences. [a]Short read sequences originating from RNA sequencing were mapped to its scaffold, and its transcript was confirmed by RT-PCR. [b]Short read sequences originating from RNA sequencing were mapped to its scaffold, but its transcript was not confirmed by RT-PCR. In BLAST-search for the transcripts, '+' and '–' indicate that deleterious mutations (premature stop codons or frameshift mutations) were absent (+) and present (–) in the sequences hit at. '+/–' indicates that we identified both transcripts without and with deleterious mutations. Species name abbreviation: *Pcha Pogonus chalceus*, *Tcas Tribolium castaneum*, *Dmel Drosophila melanogaster*

Opsin genes

One *lw opsin* gene of *T. kuznetsovi* was identified with BLAST search. The gene was divided into three genome

scaffolds and two transcript contigs (Table S2). The scaffolds and contigs were joined together using PCR and RT-PCR, and then exon and intron regions of the *lw opsin* gene were determined (Fig. 2A). The conceptually translated Lw opsin amino acid sequence was 379 residues and consisted of six exons. There was neither a premature stop codon nor a frameshift mutation in the coding sequence.

One *uv opsin* gene of *T. kuznetsovi* was identified by performing BLAST search. The gene was present within one scaffold in the genome and no contig was found in the transcripts (Table S2). The cDNA sequence of the *uv opsin* amino acid sequence was determined using RT-PCR, and then exon and intron regions of the *uv opsin* gene were determined (Fig. 2B). The conceptually translated Uv opsin amino acid sequence was 373 residues and consisted of six exons. There was neither a premature stop codon nor a frameshift mutation in the coding sequences.

Opsin phylogeny and selective pressure

A molecular phylogenetic tree of opsin genes of *T. kuznetsovi*, *P. chalceus*, *G. marinus*, *T. marmoratus* and *T. castaneum* and *A. mellifera* was reconstructed (Fig. 3, Table S4). The *lw opsin* and *uv opsin* of *T. kuznetsovi* were clustered with those of *P. chalceus*, in accordance with their taxonomic relationship. The branch length of opsin genes in *T. kuznetsovi* was not extended long.

In *lw opsin* genes, Ka/Ks ratio was 0.158131 between the sequences of the ancestor and *T. kuznetsovi* ($p = 1.12862e^{-013}$, Fisher's exact test), and Ka/Ks ratio was 0.0275072 between the sequences of the ancestor and *P. chalceus* ($p = 2.70467e^{-109}$, Fisher's exact test) (Table 3). In *uv opsin*, Ka/Ks ratio was 0.138044 between the sequences of the ancestor and *T. kuznetsovi* ($p = 1.34285e^{-024}$, Fisher's exact test), and Ka/Ks ratio was 0.0695552 between the sequences of the ancestor and *P. chalceus* ($p = 7.58434e^{-092}$, Fisher's exact test). In all of these cases, Ka/Ks ratios were far below 1.0, indicating that opsin genes have been under negative (purifying) selection in both the lineage leading to *T. kuznetsovi* and that leading to *P. chalceus.*

Subsequently, the difference in the degree of the purifying selection between the lineages from the ancestor to *T. kuznetsovi* and to *P. chalceus* was tested. According to the result of Relax analysis in Hyphy, *k* value was 0.61 ($p = 0.225$) in *lw opsin* and 2.14 ($p = 0.539$) in *uv opsin* (Table 3). Because this analysis did not show a statistical significance, we were unable to conclude whether the selection on opsin genes was relaxed or intensified in the lineage leading to *T. kuznetsovi* compared to the control lineage.

Internal structure of a compound eye

Putative photoreceptor cells stained by hematoxylin were observed in the internal structure of a vestigial compound eye in a *T. kuznetsovi* adult (Fig. 4A). The surface was covered by a transparent cuticle, a cornea. By observation from the outer surface of the head, we could see a transparent cornea and ocular ridge with black pigmentation (Fig. 1D). There was no pigmentation in cells within the eye structure, unlike compound eyes of other carabid beetles [47]. No crystalline cones or any similar structure were found [48]. An optic stalk, which is a nerve bundle connecting a compound eye and a brain, was observed [49] (Fig. 4B).

Discussion

To understand the process of subterranean colonization of organisms, the question of whether shallow subterranean habitats are a gateway to colonizing deep zones has been featured in subterranean biology [3, 4]. In the present study, we focused on a trechine beetle, *T. kuznetsovi*, which inhabits the upper hypogean zone and has a vestigial compound eye [18]. We evaluated the ability of photoreception in *T. kuznetsovi* by genomics and histological observation.

We identified one *lw opsin* gene and one *uv opsin* gene in the genome and in the transcripts in the adult. No frameshift mutation or premature stop codon was found in these exon regions, Ka/Ks ratios were significantly less than 1.0, and there was no significant difference in the selective pressure between evolutionary lineages of subterranean *T. kuznetsovi* and surface *P. chalceus*. These analyses implied that Lw opsin and Uv opsin are under

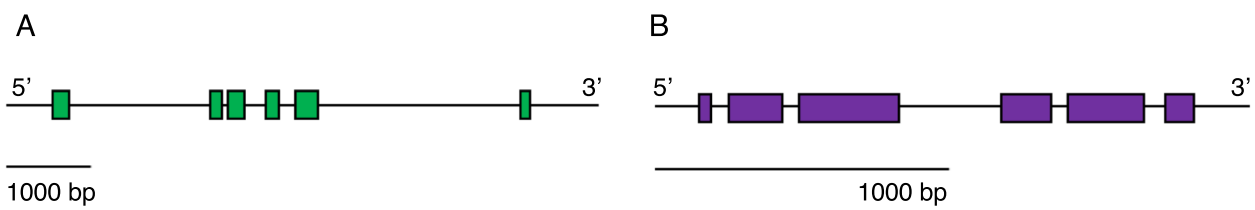

Fig. 2 The structure of opsin genes in *T. kuznetsovi*. **A** The putative structure of *lw opsin* gene, which consists of six coding exons. **B** The putative structure *uv opsin* gene, which consists of six coding exons

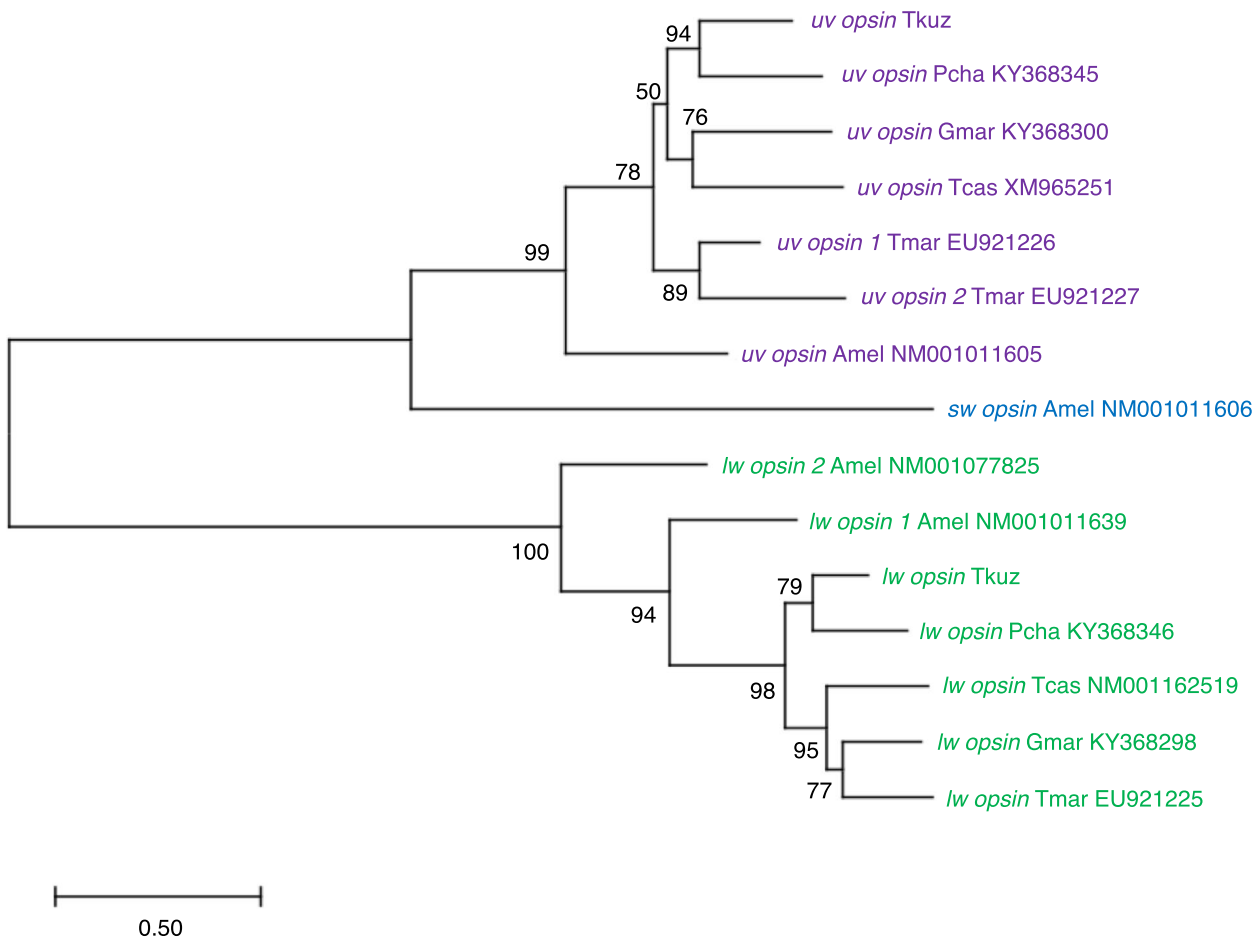

Fig. 3 A maximum likelihood tree for visual opsin genes. Bootstrap probabilities are provided on nodes. OTU names consist of the abbreviated species names, gene names and accession numbers: Tkuz, *Trechiama kuznetsovi*; Pcha, *Pogonus chalceus*; Gmar, *Gyrinus marinus*; Tmar, *Thermonectus marmoratus*; Tcas, *Tribolium castaneum*; Amel, *Apis mellifera*

Table 3 The test of selection in opsin genes of *T. kuznetsovi*

Gene	Test 1		Test 2	
	Comparison	Ka/Ks ratio	Comparison	*k* value in Relax
lw opsin	Tkuz-Ancestor	0.158131	Tkuz-Pcha	0.61
	Pcha-Ancestor	0.0275072		
uv opsin	Tkuz-Ancestor	0.138044	Tkuz-Pcha	2.14
	Pcha-Ancestor	0.0695552		

functional constraint. Transcripts of 14 phototransduction genes without deleterious mutations (premature stop codons or frameshift mutations) were detected in the assembled transcripts. One phototransduction gene, *trpl,* was found in RNA short-read sequences. These results suggested the ability of photoreception and phototransduction of *T. kuznetsovi*. In our preliminary study using LED light, we observed that adults of *T. kuznetsovi* showed clear negative phototaxis to UV light and probably also to green light (data not shown).

In subterranean diving beetles in Western Australia, the *lw opsin* gene became a pseudogene due to frameshift mutations, and neither *lw opsin* nor *uv opsin* transcripts were observed [14–16]. Frameshift mutations and premature stop codons occurred in some phototransduction genes: *Arr1*, *Arr2*, *ninaC*, *trp* and *trpl* [16]. There are two possible causes for these differences between *T. kuznetsovi* and the subterranean diving beetles. The first possibility is the difference in their ecological niches. The calcrete aquifer, in which subterranean diving beetles live, is located at a depth of 10–30 m underground [13, 50]. In contrast, the upper hypogean zone, in which *T. kuznetsovi* adults live, is a few or some dozen centimeters below the slope surface of a v-shaped valley. *Trechiama kuznetsovi* adults would occasionally be exposed to the surface due to landslides occurring as a result of precipitation or earthquakes [51–53]. This temporary light

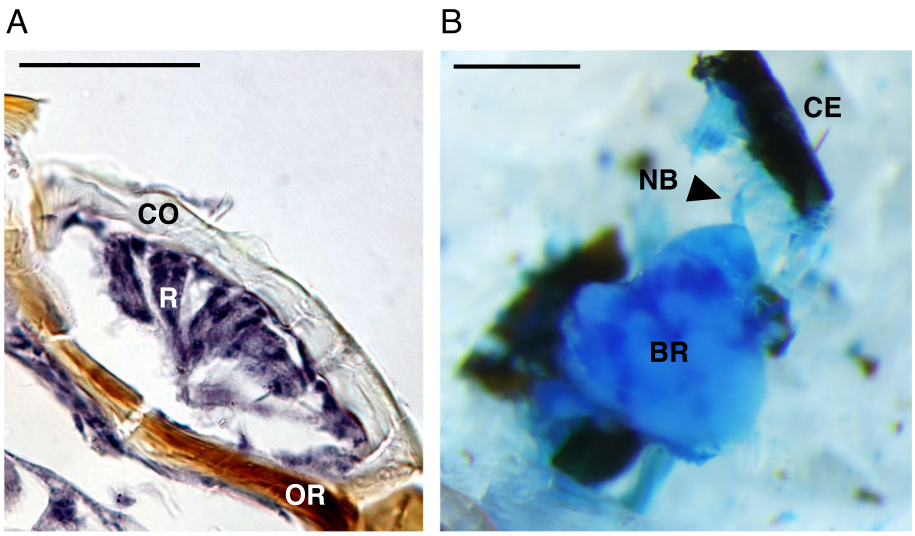

Fig. 4 The internal structure and nerve tissue of *T. kuznetsovi* head. **A** Transverse section of a compound eye, dorsal is up. Scale bar indicates 20 µm. CO, cornea; R, putative photoreceptor cells; OR, ocular ridge. **B** Dorsal view of dissected head. Nerve tissue was stained with methylene blue solution. Scale bar indicates 0.5 mm. CE, compound eye; NB, nerve bundle; BR, brain (supraesophageal ganglion)

stimulus could function as a selective pressure to retain the function of opsin genes and other phototransduction genes. For example, vestigial compound eyes could function in the response to the temporary light. Friedrich et al. [32] also suggested such a function for the retention of photoreceptor genes and phototransduction genes in *Ptomaphagus hirtus* (Leiodidae) inhabiting the Frozen Niagara cave entrance of Mammoth Cave in Kentucky, USA. Beetles in shallow subterranean environments (the upper hypogean zone and cave entrance) could tend to maintain the photoreception. The second possibility is that opsin genes and other phototransduction genes of *T. kuznetsovi* have not had enough time to become pseudogenes. However, we think this scenario is less likely because they had enough time to degenerate the eye itself. Niemiller et al. [54] showed that some cave lineages in Amblyopsidae still possess functional rhodopsin, although they inhabit an aphotic environment. This retained functionality is thought to be due to insufficient accumulation of mutations during recent subterranean colonization. As in these cave lineages, pseudogenization of opsin genes in *T. kuznetsovi* could not be observed because divergence between *T. kuznetsovi* and related terrestrial species occurred recently. To further examine this possibility, the divergence time of *Trechiama* species needs to be studied.

By performing paraffin sectioning and dissection, we observed the cells inside the compound eye and the optic stalk connecting the compound eye and the brain in *T. kuznetsovi*. These observations suggested that photoreception is structurally possible even with the vestigial compound eyes of this species. Complete loss of compound eyes and optic lobes was observed in *Sinaphaenops wangorum* (Trechinae) inhabiting the deep area of a cave in Guangxi Autonomous Region, China [55]. Thus, the existence of the optic stalk is thought to be due to the retention of photoreception ability by *T. kuznetsovi*, not to an inability of the visual system to degenerate any further.

Collectively, the results of genomics and histology analyses performed here suggested the ability of photoreception in *T. kuznetsovi*. This species is thought to possess both a surface trait (photoreception) and some subterranean traits (vestigial compound eye, underdeveloped body pigmentation and other morphological adaptations) [56, 57]. These characteristics would reflect an intermediate phase toward colonizing a deeper subterranean niche. Further understanding of the visual degeneration process will be achieved by clarifying the phylogenetic relationship between subterranean species and surface species of trechine beetles.

Conclusions

By de novo assembly of genome and transcript sequences, we identified photoreceptor genes and phototransduction genes of a trechine beetle, *Trechiama kuznetsovi*, which inhabits the upper hypogean zone. The encoded amino acid sequences of *lw opsin* and *uv opsin* had neither a premature stop codon nor a frameshift mutation, and appeared to be subject to purifying selection. We identified potential photoreceptor cells in the compound eye and nerve bundle connected to the brain. The present findings suggest that *T. kuznetsovi* has retained the ability of photoreception.

Abbreviations

Lw opsin	Long wavelength opsin
Uv opsin	Ultraviolet opsin
Arr1	Arrestin 1
Arr2	Arrestin 2
Gα49B	G protein α-subunit 49B
Gβ76C	G protein β-subunit 76C
Gγ30A	G protein γ-subunit 30A
Gprk1	G protein-coupled receptor kinase 1
InaD	Inactivation no afterpotential D
NinaA	Neither inactivation nor afterpotential A
NinaC	Neither inactivation nor afterpotential C
NorpA	No receptor potential A
Pkc53E	Protein C kinase 53E
Rab6	Rab-protein 6
RdgC	Retinal degeneration C
Trp	Transient receptor potential
Trpl	Trp-like
CO	Cornea
R	Putative photoreceptor cells
OR	Ocular ridge
CE	Compound eye
NB	Nerve bundle
BR	Brain

Supplementary Information

The online version contains supplementary material available at https://doi.org/10.1186/s40851-023-00208-7.

Additional file 1: Table S1. The result of genome and transcript sequencing in *T. kuznetsovi*.

Additional file 2: Table S2. BLAST search for opsin genes to the assembled genome and transcripts in *T. kuznetsovi*.

Additional file 3: Table S3. Primers used in PCR and RT-PCR to amplify opsin genes in *T. kuznetsovi*. *T*, annealing temperature.

Additional file 4: Table S4. BLAST search for opsin genes to non-redundant protein sequences in NCBI database.

Acknowledgements
We thank Takashi Hayakawa and Juno Shimada for technical help; Cédric Finet for technical advice; Masahiro Ôhara and Shigehisa Hori for collection site information; Elizabeth Nakajima for English editing; and members of the Koshikawa lab for sample collection and discussion. The super-computing resource was provided by Human Genome Center (the Univ. of Tokyo).

Authors' contributions
Conceptualization, T.N. and S.K.; Data acquisition, T.N., Y.T., and H.A.; Data analysis, T.N., Y.T, H.A. and S.K.; Writing, T.N. and S.K.; All authors approved the final manuscript.

Funding
This study was supported by KAKENHI (22J12200), the Sasakawa Scientific Research Grant from The Japan Science Society, Asahi Glass Foundation, Kurita Water and Environment Foundation, and the research expense fund of a Hokkaido University Ambitious Doctoral Fellowship.

Availability of data and materials
Sequence reads and scaffolds of the genome and transcripts of *Trechiama kuznetsovi* were deposited to DDBJ/EMBL/GenBank (DRR415324, DRR415325, PRJDB15628 and PRJDB15666).

Declarations

Ethics approval and consent to participate
Not applicable.

Consent for publication
Not applicable.

Competing interests
The authors declare no competing interests.

Received: 28 February 2023 Accepted: 21 April 2023
Published online: 12 May 2023

References

1. McGaugh SE, Gross JB, Aken B, Blin M, Borowsky R, Chalopin D, et al. The cavefish genome reveals candidate genes for eye loss. Nat Commun. 2014;5:1–10. https://doi.org/10.1038/ncomms6307.
2. Mammola S, Cardoso P, Culver DC, Deharveng L, Ferreira RL, Fišer C, et al. Scientists' warning on the conservation of subterranean ecosystems. Bioscience. 2019;69:641–50. https://doi.org/10.1093/biosci/biz064.
3. Mammola S, Amorim IR, Bichuette ME, Borges PAV, Cheeptham N, Cooper SJB, et al. Fundamental research questions in subterranean biology. Biol Rev. 2020;95:1855–72. https://doi.org/10.1111/brv.12642.
4. Culver DC, Pipan T. Superficial subterranean habitats – gateway to the subterranean realm. Cave Karst Sci. 2009;35:5–12.
5. Soares D, Niemiller ML. Sensory adaptations of fishes to subterranean environments. Bioscience. 2013;63:274–83. https://doi.org/10.1525/bio.2013.63.4.7.
6. Jeffery WR. Regressive evolution in *Astyanax* cavefish. Annu Rev Genet. 2009;43:25–47. https://doi.org/10.1146/annurev-genet-102108-134216.
7. Friedrich M. Biological clocks and visual systems in cave-adapted animals at the dawn of speleogenomics. Integr Comp Biol. 2013;53:50–67. https://doi.org/10.1093/icb/ict058.
8. Simon N, Fujita S, Porter M, Yoshizawa M. Expression of extraocular opsin genes and light-dependent basal activity of blind cavefish. PeerJ. 2019;7:e8148. https://doi.org/10.7717/peerj.8148.
9. Policarpo M, Fumey J, Lafargeas P, Naquin D, Thermes C, Naville M, et al. Contrasting gene decay in subterranean vertebrates: insights from cavefishes and fossorial mammals. Mol Biol Evol. 2021;38:589–605. https://doi.org/10.1093/molbev/msaa249.
10. Yamamoto Y, Jeffery WR. Central role for the lens in cave fish eye degeneration. Science. 2000;289:631–3. https://doi.org/10.1126/science.289.5479.631.
11. David-Gray ZK, Bellingham J, Munoz M, Avivi A, Nevo E, Foster RG. Adaptive loss of ultraviolet-sensitive/violet-sensitive (UVS/VS) cone opsin in the blind mole rat (*Spalax ehrenbergi*). Eur J Neurosci. 2002;16:1186–94. https://doi.org/10.1046/j.1460-9568.2002.02161.x.
12 Gower DJ, Fleming JF, Pisani D, Vonk FJ, Kerkkamp HMI, Peichl L, et al. Eye-transcriptome and genome-wide sequencing for Scolecophidia: implications for inferring the visual system of the ancestral snake. Genome Biol Evol. 2021;13:evab253. https://doi.org/10.1093/gbe/evab253.
13. Tierney SM, Langille B, Humphreys WF, Austin AD, Cooper SJB. Massive parallel regression: a précis of genetic mechanisms for vision loss in diving beetles. Integr Comp Biol. 2018;58:465–79. https://doi.org/10.1093/icb/icy035.
14. Tierney SM, Cooper SJB, Saint KM, Bertozzi T, Hyde J, Humphreys WF, et al. Opsin transcripts of predatory diving beetles: a comparison of surface and subterranean photic niches. R Soc Open Sci. 2015;2:140386. https://doi.org/10.1098/rsos.140386.
15. Langille BL, Hyde J, Saint KM, Bradford TM, Stringer DN, Tierney SM, et al. Evidence for speciation underground in diving beetles (Dytiscidae) from a subterranean archipelago. Evolution. 2021;75:166–75. https://doi.org/10.1111/evo.14135.
16. Langille BL, Tierney SM, Bertozzi T, Beasley-Hall PG, Bradford TM, Fagan-Jeffries EP, et al. Parallel decay of vision genes in subterranean water beetles. Mol Phylogenet Evol. 2022;173:107522. https://doi.org/10.1016/j.ympev.2022.107522.
17. Ortuño VM, Cuesta E, Gilgado JD, Ledesma E. A new hypogean *Trechus* Clairville (Coleoptera, Carabidae, Trechini) discovered in a non-calcareous superficial subterranean habitat of the Iberian system (Central Spain). Zootaxa. 2014;3802:359–72. https://doi.org/10.11646/zootaxa.3802.3.5.

18. Uéno SI, Lafer GS. A new anophthalmic *Trechiama* (Coleoptera, Trechinae) from Central Hokkaido, Northeast Japan. Elytra. 1992;20:137–43.
19. Chen S, Zhou Y, Chen Y, Gu J. fastp: an ultra-fast all-in-one FASTQ preprocessor. Bioinformatics. 2018;34:i884–90. https://doi.org/10.1093/bioinformatics/bty560.
20. Bolger AM, Lohse M, Usadel B. Trimmomatic: a flexible trimmer for Illumina sequence data. Bioinformatics. 2014;30:2114–20. https://doi.org/10.1093/bioinformatics/btu170.
21. Chikhi R, Medvedev P. Informed and automated *k*-mer size selection for genome assembly. Bioinformatics. 2014;30:31–7. https://doi.org/10.1093/bioinformatics/btt310.
22. Kajitani R, Toshimoto K, Noguchi H, Toyoda A, Ogura Y, Okuno M, et al. Efficient de novo assembly of highly heterozygous genomes from whole-genome shotgun short reads. Genome Res. 2014;24:1384–95. https://doi.org/10.1101/gr.170720.113.
23. Grabherr MG, Haas BJ, Yassour M, Levin JZ, Thompson DA, Amit I, et al. Full-length transcriptome assembly from RNA-Seq data without a reference genome. Nat Biotechnol. 2011;29:644–52. https://doi.org/10.1038/nbt.1883.
24. Haas BJ, Papanicolaou A, Yassour M, Grabherr M, Blood PD, Bowden J, et al. *De novo* transcript sequence reconstruction from RNA-seq using the Trinity platform for reference generation and analysis. Nat Protoc. 2013;8:1494–512. https://doi.org/10.1038/nprot.2013.084.
25. Van Belleghem SM, Vangestel C, De Wolf K, De Corte Z, Möst M, Rastas P, et al. Evolution at two time frames: polymorphisms from an ancient singular divergence event fuel contemporary parallel evolution. PLoS Genet. 2018;14:e1007796. https://doi.org/10.1371/journal.pgen.1007796.
26. Nishimura O, Hara Y, Kuraku S. gVolante for standardizing completeness assessment of genome and transcriptome assemblies. Bioinformatics. 2017;33:3635–7. https://doi.org/10.1093/bioinformatics/btx445.
27. Shen W, Le S, Li Y, Hu F. SeqKit: a cross-platform and ultrafast toolkit for FASTA/Q file manipulation. PLoS One. 2016;11:e0163962. https://doi.org/10.1371/journal.pone.0163962.
28. Kim D, Langmead B, Salzberg SL. HISAT: a fast spliced aligner with low memory requirements. Nat Methods. 2015;12:357–60. https://doi.org/10.1038/nmeth.3317.
29. Thorvaldsdóttir H, Robinson JT, Mesirov JP. Integrative Genomics Viewer (IGV): high-performance genomics data visualization and exploration. Brief Bioinform. 2013;14:178–92. https://doi.org/10.1093/bib/bbs017.
30. Sharkey CR, Fujimoto MS, Lord NP, Shin S, McKenna DD, Suvorov A, et al. Overcoming the loss of blue sensitivity through opsin duplication in the largest animal group, beetles. Sci Rep. 2017;7:8. https://doi.org/10.1038/s41598-017-00061-7.
31. Bao R, Friedrich M. Molecular evolution of the *Drosophila* retinome: exceptional gene gain in the higher Diptera. Mol Biol Evol. 2009;26:1273–87. https://doi.org/10.1093/molbev/msp039.
32. Friedrich M, Chen R, Daines B, Bao R, Caravas J, Rai PK, et al. Phototransduction and clock gene expression in the troglobiont beetle *Ptomaphagus hirtus* of Mammoth cave. J Exp Biol. 2011;214:3532–41. https://doi.org/10.1242/jeb.060368.
33. Tsuji T, Gotoh H, Morita S, Hirata J, Minakuchi Y, Yaginuma T, et al. Molecular characterization of eye pigmentation-related ABC transporter genes in the ladybird beetle *Harmonia axyridis* reveals striking gene duplication of the white gene. Zool Sci. 2018;35:260–7. https://doi.org/10.2108/zs170166.
34. Futahashi R, Kawahara-Miki R, Kinoshita M, Yoshitake K, Yajima S, Arikawa K, et al. Extraordinary diversity of visual opsin genes in dragonflies. Proc Natl Acad Sci USA. 2015;112:E1247–56. https://doi.org/10.1073/pnas.1424670112.
35. Guignard Q, Allison JD, Slippers B. The evolution of insect visual opsin genes with specific consideration of the influence of ocelli and life history traits. BMC Ecol Evol. 2022;22:2. https://doi.org/10.1186/s12862-022-01960-8.
36. Leung NY, Montell C. Unconventional roles of opsins. Annu Rev Cell Dev Biol. 2017;33:241–64. https://doi.org/10.1146/annurev-cellbio-100616-060432.
37. Leung NY, Thakur DP, Gurav AS, Kim SH, Pizio AD, Niv MY, et al. Functions of opsins in *Drosophila* taste. Curr Biol. 2020;30:1367-79.e6. https://doi.org/10.1016/j.cub.2020.01.068.
38. Conesa A, Madrigal P, Tarazona S, Gomez-Cabrero D, Cervera A, McPherson A, et al. A survey of best practices for RNA-seq data analysis. Genome Biol. 2016;17:13. https://doi.org/10.1186/s13059-016-0881-8.
39. Slater GSC, Birney E. Automated generation of heuristics for biological sequence comparison. BMC Bioinf. 2005;6:1–11. https://doi.org/10.1186/1471-2105-6-31.
40. Smith AF, Posakony JW, Rebeiz M. Automated tools for comparative sequence analysis of genic regions using the GenePalette application. Dev Biol. 2017;429:158–64. https://doi.org/10.1016/j.ydbio.2017.06.033.
41. Tamura K, Stecher G, Kumar S. MEGA11: molecular evolutionary genetics analysis version 11. Mol Biol Evol. 2021;38:3022–7. https://doi.org/10.1093/molbev/msab120.
42. Goldman N, Yang Z. A codon-based model of nucleotide substitution for protein-coding DNA sequences. Mol Biol Evol. 1994;11:725–36. https://doi.org/10.1093/oxfordjournals.molbev.a040153.
43 Zhang Z. KaKs_Calculator 30: calculating selective pressure on coding and non-coding sequences. Genom Proteom Bioinform. 2022;20:536–40. https://doi.org/10.1016/j.gpb.2021.12.002.
44. Wertheim JO, Murrell B, Smith MD, Kosakovsky Pond SL, Scheffler K. RELAX: detecting relaxed selection in a phylogenetic framework. Mol Biol Evol. 2015;32:820–32. https://doi.org/10.1093/molbev/msu400.
45. Cornette R, Matsumoto T, Miura T. Histological analysis of fat body development and molting events during soldier differentiation in the damp-wood termite, *Hodotermopsis sjostedti* (Isoptera, Termopsidae). Zool Sci. 2007;24:1066–74. https://doi.org/10.2108/zsj.24.1066.
46. Oguchi K, Miura T. Unique morphogenesis in the damp-wood termite: abscission of the stylus during female reproductive caste differentiation. Zool Sci. 2019;36:380–6. https://doi.org/10.2108/zs190056.
47. Home EM. The fine structure of some carabid beetle eyes, with particular reference to ciliary structures in the retinula cells. Tissue Cell. 1976;8:311–33. https://doi.org/10.1016/0040-8166(76)90055-0.
48. van der Kooi CJ, Stavenga DG, Arikawa K, Belušič G, Kelber A. Evolution of insect color vision: from spectral sensitivity to visual ecology. Annu Rev Entomol. 2021;66:435–61. https://doi.org/10.1146/annurev-ento-061720-071644.
49. Whited JL, Cassell A, Brouillette M, Garrity PA. Dynactin is required to maintain nuclear position within postmitotic *Drosophila* photoreceptor neurons. Development. 2004;131:4677–86. https://doi.org/10.1242/dev.01366.
50. Langille BL, Tierney SM, Austin AD, Humphreys WF, Cooper SJB. How blind are they? Phototactic responses in stygobiont diving beetles (Coleoptera: Dytiscidae) from calcrete aquifers of Western Australia. Austral Entomol. 2019;58:425–31. https://doi.org/10.1111/aen.12330.
51. Dhakal A, Tsuchiya S, Ohsaka O. Long term change in landslide area in Ikawa Lake catchment using aerial photographs and GIS. J Erosion Contr. 2007;59:25–31. https://doi.org/10.11475/sabo1973.59.6_25.
52 Tsuchiya S, Imaizumi F. Large sediment movement caused by the catastrophic Ohya-kuzure landslide. J Disaster Res. 2010;5:257–63. https://doi.org/10.20965/jdr.2010.p0257.
53. Matsuoka N, Imaizumi F, Nishii R. Geomorphic dynamics and sediment budget in the southern Japanese Alps: recent studies and prospects. J Geogr. 2013;122:591–614. https://doi.org/10.5026/jgeography.122.591.
54. Niemiller ML, Fitzpatrick BM, Shah P, Schmitz L, Near TJ. Evidence for repeated loss of selective constraint in rhodopsin of amblyopsid cavefishes (Teleostei: Amblyopsidae). Evolution. 2013;67:732–48. https://doi.org/10.1111/j.1558-5646.2012.01822.x.
55. Luo XZ, Wipfler B, Ribera I, Liang HB, Tian MY, Ge SQ, et al. The cephalic morphology of free-living and cave-dwelling species of trechine ground beetles from China (Coleoptera, Carabidae). Org Divers Evol. 2018;18:125–42. https://doi.org/10.1007/s13127-017-0351-5.
56. Protas M, Jeffery WR. Evolution and development in cave animals: from fish to crustaceans. Wiley Interdiscip Rev Dev Biol. 2012;1:823–45. https://doi.org/10.1002/wdev.61.
57. Bilandžija H, Laslo M, Porter ML, Fong DW. Melanization in response to wounding is ancestral in arthropods and conserved in albino cave species. Sci Rep. 2017;7:1–11. https://doi.org/10.1038/s41598-017-17471-2.

Publisher's Note